Electronic Materials Letters, Vol. 2, No. 2 (2006), pp. 107-110

Bistable Resistance Switching Behaviors of SiO_2 and TiO_2 Binary Metal Oxide Films

In-Sung Park[1], Kyong-Rae Kim[2], Young-Soon Kim[3], and Jinho Ahn[3,*]

[1]Information Display Research Institute, Hanyang University, Seoul 133-791, Korea
[2]Department of Information Display Engineering, Hanyang University, Seoul 133-791, Korea
[3]Department of Materials Science and Engineering, Hanyang University, Seoul 133-791, Korea

The bistable resistance switching characteristics of amorphous SiO_2 and poly-crystalline TiO_2 were investigated using Pt top and bottom electrodes sandwiched structure. Both films exhibit well defined switching characteristics. All device operation characteristic parameters such as forming, reset, and set voltages of TiO_2 are distinctly smaller than those of SiO_2, indicating that the values of these parameters can be related to the dielectric constant. From I-V curve analyses, it is found that the low resistance states of both films obey an ohmic conduction mechanism and the high resistance states show generation of a Schottky potential barrier. Regarding the mechanism for resistance switching of the binary oxide, it is suggested that the generation and annihilation of potential barriers accounts for the changes to the high resistance state and low resistance state, respectively.

Keywords: resistance switching, binary metal oxide, SiO_2, TiO_2

1. INTRODUCTION

Insulating binary oxides have attracted considerable interest with regard to their application as nonvolatile memory elements, the key technology for modern mobile electronic devices. In terms of meeting the requirements for next generation advanced devices, resistance random access memory (ReRAM) offers suitable properties such as low power consumption, high density, and high operation speed[1,2]. This memory is based on the resistance switching behaviors of insulators sandwiched between metal electrodes. Resistance switching phenomena have been found in various types of insulators including binary metal oxides[3-5], perovskite-type oxides[6], and even organic materials[7].

The choice of insulator is an important parameter for the device application, since the resistance switching characteristics depend on the energy bandgap and the dielectric constant of the insulator[8]. Binary oxide offers several advantages such as precise composition control and film quality with minimum complexity. The switching behaviors of a number of binary oxides have been widely investigated since the 1960s, and those of transition metal oxides including NiO[3,4] and TiO_2[5] have attracted interest because their switching properties are more universal than those of perovskite materials.

Titanium dioxide (TiO_2) is a versatile material that forms in a number of crystalline phases. For example, crystallized anatase TiO_2 has a very large dielectric constant of more than 60 but a small bandgap of 3 eV. In contrast, silicon dioxide (SiO_2) is a widely employed material in electronics with a low dielectric constant of 3.9 and a high bandgap of 9 eV. A comparison of the universal resistance switching behavior of these two metal oxides, i.e., amorphous SiO_2 and poly-crystalline TiO_2 films, having extremely different bandgaps and dielectric constants, would provide useful information for future research and applications. In this paper, the switching characteristics including operation voltage and resistance ratio of SiO_2 and TiO_2 films are discussed and the conduction mechanisms for bistable resistance states based on ohmic conduction and potential barrier are proposed.

2. EXPERIMENTAL

Bottom Pt electrode deposition was carried out on a p-type Si(100) wafer using a dc magnetron sputtering system with 4-inch diameter targets (99.95% purity). Two insulating SiO_2 and TiO_2 films were then deposited by the RF magnetron sputter system. The Pt top electrode was also deposited with the same fabrication process as the bottom electrode. All deposition processes were performed at room temperature with a base pressure of less than 1×10^{-6} Torr. Deposited

*Corresponding author: jhahn@hanyang.ac.kr

insulators and electrodes were all 40 nm thick. Electrode patterning was performed by the conventional liftoff method. The resistance switching was measured using an HP4155A semiconductor parameter analyzer. This measurement was conducted in voltage sweep mode with current compliance at room temperature. If the devices failed to exhibit switching behaviors, a thermal annealing process in N_2 ambient was executed until resistance switching behavior appeared. Depth profile analyses using Auger electron spectroscopy (AES) and X-ray diffraction (XRD) were performed in order to identify the composition and crystalline structure of the insulators, respectively.

3. RESULTS AND DISCUSSION

The depth profiles of the devices with SiO_2 film after deposition are shown in Fig. 1(a). It is clear that the SiO_2 film is well defined on the bottom electrode. The amounts of silicon and oxygen in the insulators remain constant along their depths. For the SiO_2 and TiO_2 films, the resistance switching characteristics begin to appear after the annealing process at 500 and 800 °C, respectively. The crystalline structures identified by XRD were amorphous SiO_2 and poly-crystalline TiO_2 with a mixture of anatase and rutile phases after their respective annealing processes, as shown in Fig. 1(b). Recently, it has been reported that TiO_2 anatase nano-crystal plays a major role in high speed switching[9].

The bistable resistance switching behaviors of annealed SiO_2 and TiO_2 films including the forming process are presented in Figs. 2(a) and 2(b), respectively. First, a forming process is needed to bring about the resistance switching. This is accomplished by increasing the bias along the insulator until dielectric breakdown occurs. By setting the current compliance, the insulator breakdown is reversibly controlled at the breakdown voltage (V_f). The values of V_f are 18.1 and 6.1 V for SiO_2 and TiO_2 films, respectively, as shown in Fig. 2. For the forming process, a model has been proposed wherein a conducting filament forms as a leakage path in the

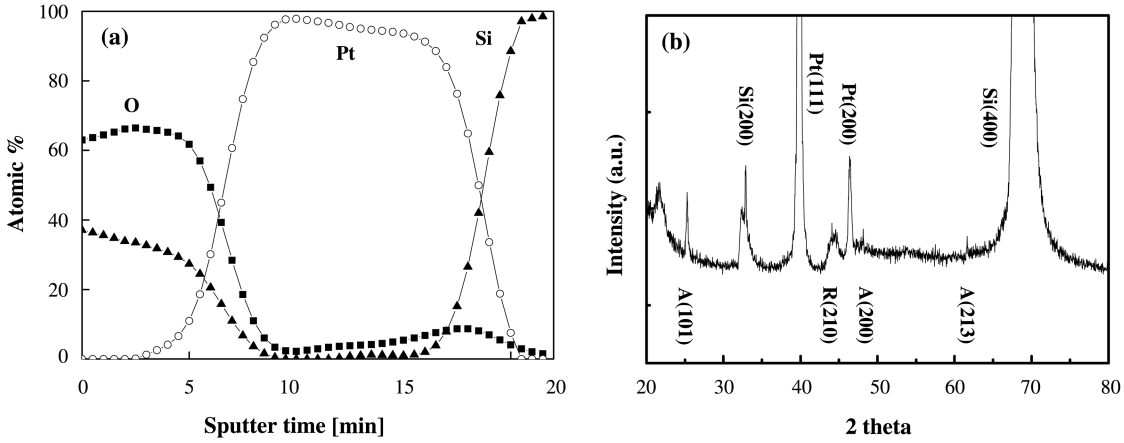

Fig. 1. (a) AES depth profiles of SiO_2 film and (b) XRD spectrum of TiO_2 film. (A: anatase, R: rutile).

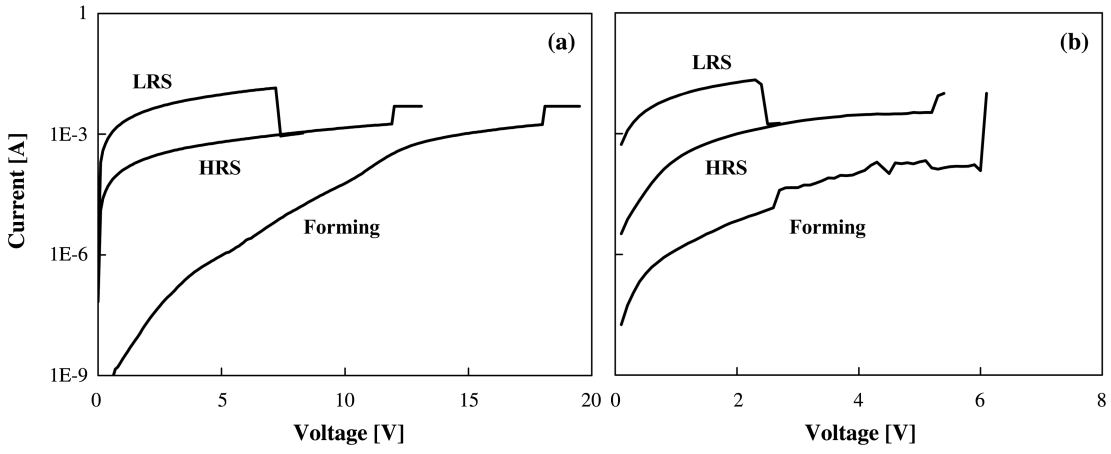

Fig. 2. I-V curves showing resistance switching behaviors of (a) SiO_2 and (b) TiO_2 films.

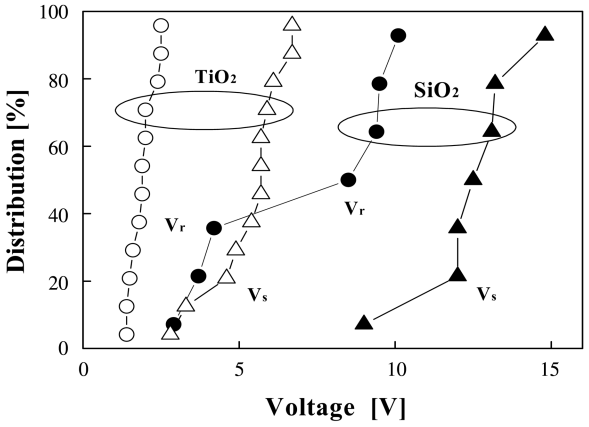

Fig. 3. Distribution of switching characteristic voltages for SiO_2 and TiO_2 films.

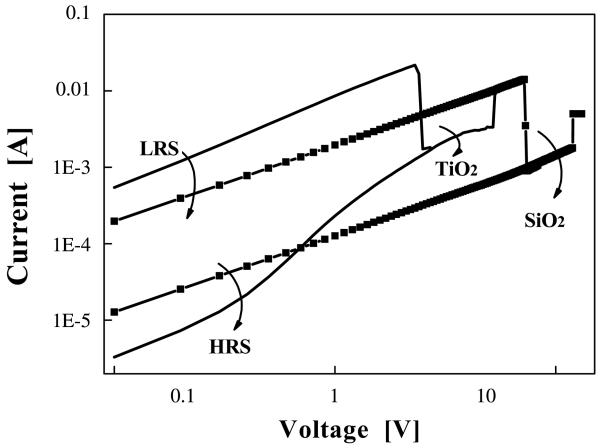

Fig. 4. I-V curves of SiO_2 and TiO_2 films plotted in log-log scales.

insulator[10]. After the forming process, another voltage sweep was done for the resistance switching. The switching characteristic indicates that the insulator exhibits both a low resistance state (LRS) and a high resistance state (HRS), and these two different states are observed repeatedly by external voltage stress. The LRS with high current conduction is generally induced first by a voltage sweep. The film shows a sudden precipitation of current at a certain voltage (V_r), where the current level is maximum. In order to switch the LRS to a HRS without hard breakdown, it is necessary to cut the application of voltage immediately after negative differential resistance (NDR) occurs. The current increase rate for the subsequent voltage sweep is slower than that of the LRS. The current is also restricted at another breakdown voltage (V_s), which is usually lower than V_f with the same current compliance. The resistance states can be repeated by voltage sweeping with slight variation of the values of V_r and V_s.

The characteristic voltages V_r and V_s for both films are shown in Fig. 3. It is observed that the values of V_r are always lower than those of V_s for both specimens. The values of V_r and V_s for TiO_2 film are higher than those of SiO_2. This indicates that the voltage with maximum current, which is similar to V_r, is related to the dielectric constant of amorphous oxides[8]. It was also reported that V_r and V_s for NiO films increases due to the presence of fewer defects at the high deposition temperature. This gives mobility to the molecules and makes them spatially stable[4]. The switching voltages of TiO_2 film in this study are somewhat higher than those previously reported[5]. It is suspected that the higher switching voltages obtained here may be related to the dielectric constant of the insulator.

The analysis of the I-V curves may provide some insight concerning the bulk properties of insulators or surface states at the electrode, which give rise to the switching behavior. For this purpose, the LRS and HRS are redrawn as log-log plots in Fig. 4. For the LRS, both films have slopes of unity up to V_r, implying ohmic behaviors. The resistance values for SiO_2 and TiO_2 films at the LRS are 510 and 52 Ω while the bandgap energy values are 9 and 3 eV, respectively. Meanwhile, it is evident that HRS shows ohmic behavior only in a very low voltage region. For most voltage regions of TiO_2, the current deviates from the linear dependency. For the conduction mechanism at the HRS, many researchers have proposed the rupture of conducting filaments[10]. Recently, Choi. *et al.* suggested that the resistive switching in TiO_2 film is closely related to the formation and rupture of conducting filaments, where joule heating from the current causes local rupturing of filaments[11]. Even if the number of filaments at the HRS is smaller than that of the LRS, the current should obey ohmic conduction through the remaining filaments. However, ohmic behavior at the HRS occurs only in a limited voltage region, indicating that an additional conduction mechanism plays a role in the resistance change at the HRS.

The non-linear I-V curves at the high voltage regions of the HRS suggest the generation of a Schottky potential barrier. Regardless of whether the conduction mechanism of the insulator is electrode-limited or bulk-limited, the potential barrier works to hinder the charge carriers from flowing from one electrode to the other. It is thought that a negative resistance phenomenon at the LRS triggers the redistribution of charge carriers and subsequently generates potential barriers. Therefore, the I-V curve of the LRS after NDR becomes similar to that of the HRS due to the generation of potential barrier. From these results, we hypothesize that the generation and annihilation of a potential barrier may be responsible for the switching mechanism. The soft breakdown at the HRS causes the filaments to form a bridge between the top and bottom electrodes. As a result, the charges can move freely with low resistance due to the annihilation of the potential barrier. The NDR at the LRS results in charge redistribution and potential barrier is subsequently generated

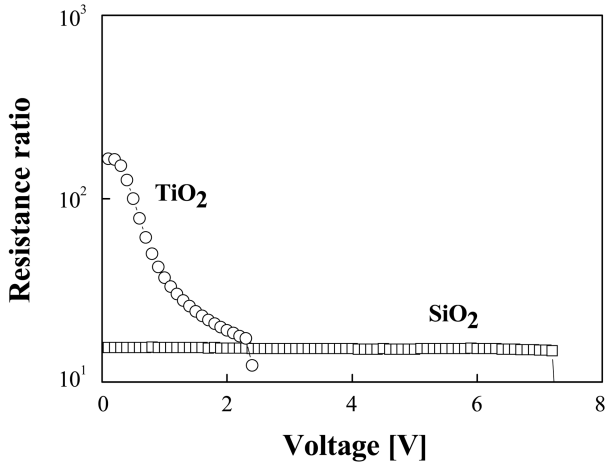

Fig. 5. Dynamic resistance ratio for SiO_2 and TiO_2 films.

near the electrode with or without any other traps in the bulk insulator. The generation of the potential barrier prevents the charge flow and thus causes switching to the HRS.

As the HRS current is non-linear, the dynamic resistance ratios (R_{HRS}/R_{LRS}) for SiO_2 and TiO_2 films are shown in Fig. 5. The ratio for SiO_2 is constant and close to 15 due to the ohmic behavior of HRS until reaching V_r. The resistance ratio of TiO_2 is enhanced by 1 order of magnitude compared to SiO_2. However, the resistance ratio of TiO_2 is voltage dependent due to its early deviation from ohmic conduction at the HRS, and decreases with applied voltage. As lower operation voltage is required, a high resistance ratio is obtained with TiO_2 films.

4. CONCLUSIONS

The resistance switching characteristics of amorphous SiO_2 and poly-crystalline TiO_2 were investigated and compared for an MIM structure with symmetric Pt electrodes. The device operation parameters such as forming, reset, and set voltages of TiO_2 are distinctly reduced relative to those of SiO_2, thus indicating the values of these parameters decrease with the dielectric constant of the film. From analyses of I-V curves, it was found that the LRSs of both films obey an ohmic conduction mechanism with resistance values of 510 and 52 Ω, respectively. However, the HRSs show non-linear I-V curves at high voltage regions, suggesting the generation of a Schottky potential barrier. Regarding the mechanism for resistance switching of the binary oxide, it is suggested that the generation and annihilation of potential barriers accounts for the changes to the high resistance state and low resistance state, respectively. In spite of a decrease of dynamic ratios with voltage, lower operation voltage with a high resistance ratio is obtained with TiO_2 films. The physical properties and switching mechanisms that impact ReRAM element operation should be further investigated for next generation nonvolatile memory.

ACKNOWLEDGEMENTS

This study was supported by "The National research program for the 0.1 Terabit Non-Volatile Memory Development sponsored by Korea Ministry of Commerce, Industry and Energy" and by the Korea Research Foundation Grant funded by the Korean Government (MOEHRD) (KRF-2005- 005-D00165).

REFERENCES

1. Q. Liu, N. J. Wu, and Ignatiev, *Appl. Phys. Lett.* **76**, 2749 (2000).
2. I. G. Baek, M. S. Lee, S. Seo, M. J. Lee, D. H. Seo, D.-S Suh, J. C. Park, S. O. Park, H. S. Kim, I. K. Yoo, U.-I. Chung, and J. T. Moon, *International Electron Devices Meeting*, p.587, San Francisco, CA (2004).
3. S. Seo, M. J. Lee, D. H. Seo, E. J. Jeoung, D.-S. Suh, Y. S. Joung, I. K. Yoo, I. R. Hwang, S. H. Kim, I. S. Byun, J.-S. Kim, J. S. Choi, and B. H. Park, *Appl. Phys. Lett.* **85**, 5655 (2004).
4. J.-W. Park, J.-W. Park, D.-Y. Kim, and J.-K. Lee, *J. Vac. Sci. Technol. A* **23**, 1309 (2005).
5. C. Rohde, B. J. Choi, D. S. Jeong, S. Choi, J.-S. Zhao, and C. S. Hwang, *Appl. Phys. Lett.* **86**, 262907 (2005).
6. Y. Watanabe, J. G. Bednorz, A. Bietsch, Ch Gerber, D. Widmer, A. Beck, and S. J. Wind, *Appl. Phys. Lett.* **78**, 3738 (2001).
7. A. K. Mahapatro, R. Agrawal, and S. Ghosh, *J. Appl. Phys.* **96**, 3583 (2004).
8. G. Dearnaley, A. M. Stoneham, and D. V. Morgan, *Rep. Prog. Phys.* **33**, 1129, (1970).
9. M. Fujimoto, H. Koyama, Y. Hosoi, K. Ishihara, and S. Kobayashi, *Jpn. J. Appl. Phys.* **45**, L310 (2006).
10. G. Dearnaley, D. V. Morgan, and A. M. Stoneham, *J. Non-Cryst. Solids* **4**, 593 (1970).
11. B. J. Choi, D. S. Jeong, S. K. Kim, S. Choi, J. H. Oh, C. Rohde, H. J. Kim, C. S. Hwang, K. Szot, R. Waser, B. Reichenberg, and S. Tiedke, *J. Appl. Phys.* **98**, 033715 (2005).